Supporting Information

Water-Floating Giant Nanosheets from Helical Peptide Pentamers

Jaehun Lee[1†], Ik Rang Choe[1†], Nak-Kyoon Kim[3], Won-Je Kim[3], Hyung-Seok Jang[2], Yoon-Sik Lee[2], and Ki Tae Nam[1]*

[1]Department of Materials Science and Engineering, Seoul National University, Seoul 151-748, Korea

[2]School of Chemical and Biological Engineering, Seoul National University, Seoul 151-748, Korea

[3]Advanced Analysis Center, Korea Institute of Science and Technology (KIST), Seoul 136-791, Korea

*Corresponding author:

Prof. Ki Tae Nam

E-mail: nkitae@snu.ac.kr

Seoul National University, Korea

Supporting Figures & Tables

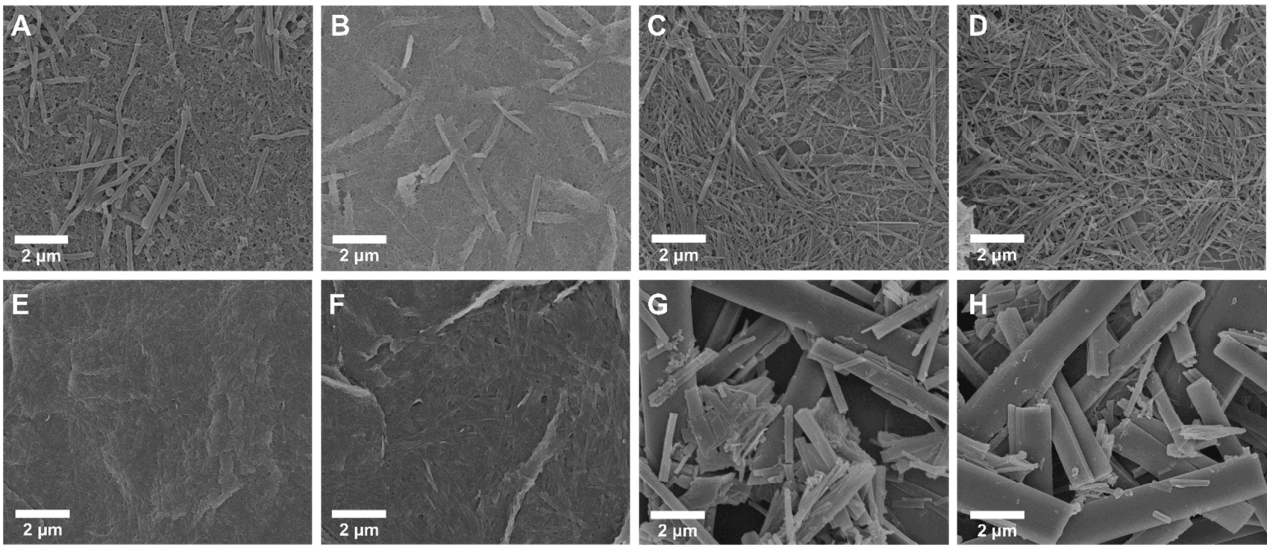

Figure S1. SEM images of self-assembled peptides in water droplets (A) 30 min incubated FYCYF (B) 120 h incubated FYCYF (C) 30 min incubated YFCYF (D) 120 h incubated YFCYF (E) 30 min incubated FYCFY (F) 120 h incubated FYCFY (G) 30 min incubated FFCFF (H) 120 h incubated FFCFF

Table S1. Sequences dependent self-assembly at the air/water interface

Sequence	Incubation time at 80°C	
	30 min	120 hour
FYCYF	aggregations 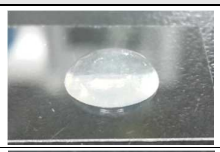	thin film at the air/water interface 
YFCYF	aggregations 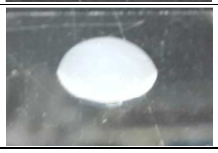	aggregations 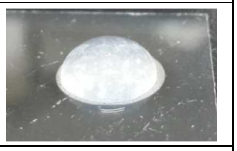
FYCFY	wrinkled film at the air/water interface 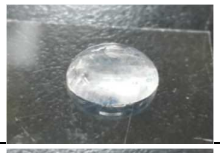	wrinkled film at the air/water interface 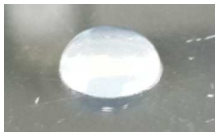
FFCFF	aggregations 	aggregations 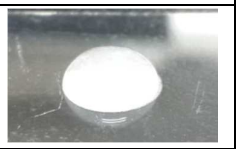

Table S2. Facet formation of YFCFY dimer depending on buffer conditions

Buffer (pH 7)	Concentration			
	50 mM	100 mM	300 mM	500 mM
HEPES	Faceting	Faceting	Faceting	No faceting
Sodium phosphates	Faceting	Faceting	Faceting	No faceting
Sodium citrates	Faceting	Faceting	No faceting	No faceting

Monomer YFCFY was fully oxidized into dimer form in pure water, then the solution was dried up by lyophilization to get pure dimer peptide. The dimer peptide was dissolved in each buffer solution and its concentration was 0.5 mM. As shown in Table S2, faceting phenomenon does not occur when the buffer concentration is too high. It means that the ions in the buffer partially screen charges of the peptide, resulting inhibition of the self-assembly into large sheets. However, YFCFY can assemble into rigid sheets in several kinds of buffers over a wide range of buffer concentration.

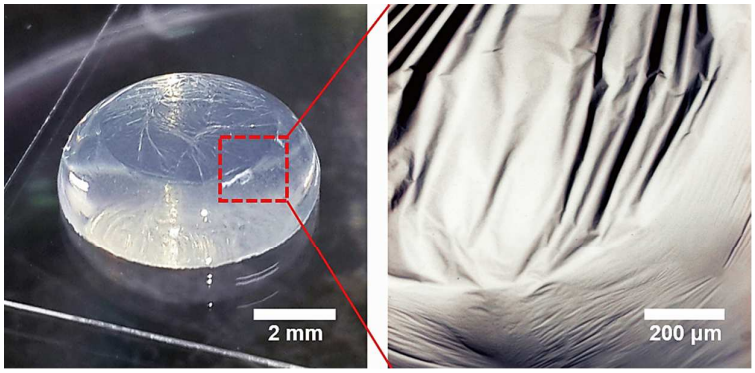

Figure S2. Optical microscopy image of the faceted droplet (left). The edge was magnified (right) and the image revealed that the unbroken giant sheet was formed on the droplet.

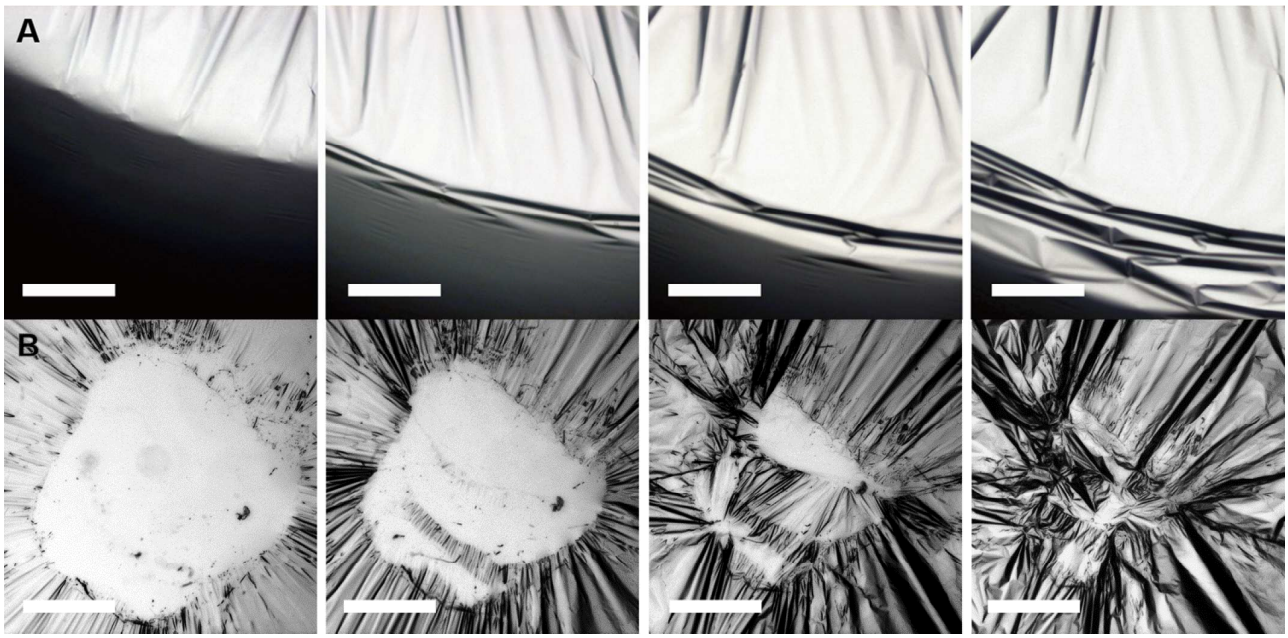

Figure S3. Series of in-situ optical microscopy images. During the facet formation, expansion of the peptide sheet in edge of the droplet was observed (A). After top of the droplet was broken with a syringe, the surface was recovered (B) within 15 min. All the scale bar is 200 micrometers.

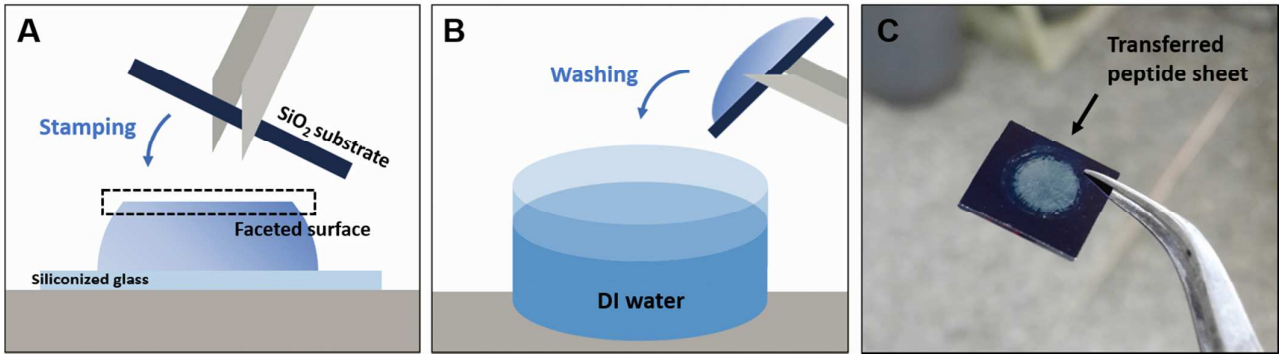

Figure S4. Stamping method. Faceted surface was transferred to the silicone oxide substrate by stamping (A). After that, remaining fibril and fragment were removed by washing the sample with deionized water (B) and dried (C).

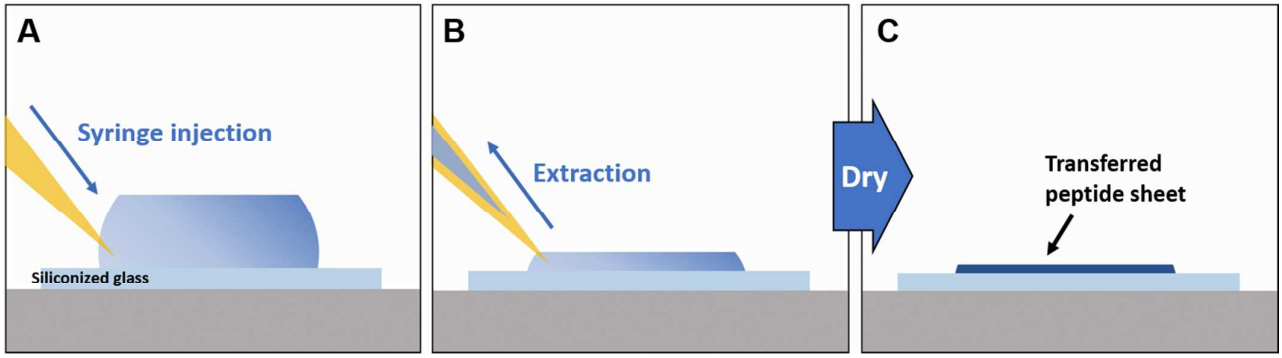

Figure S5. Extraction method. A syringe was inserted carefully into faceted droplet (A). The Inner solution of the droplet was extracted slowly as maintaining sheet on the top (B) and dried (C).

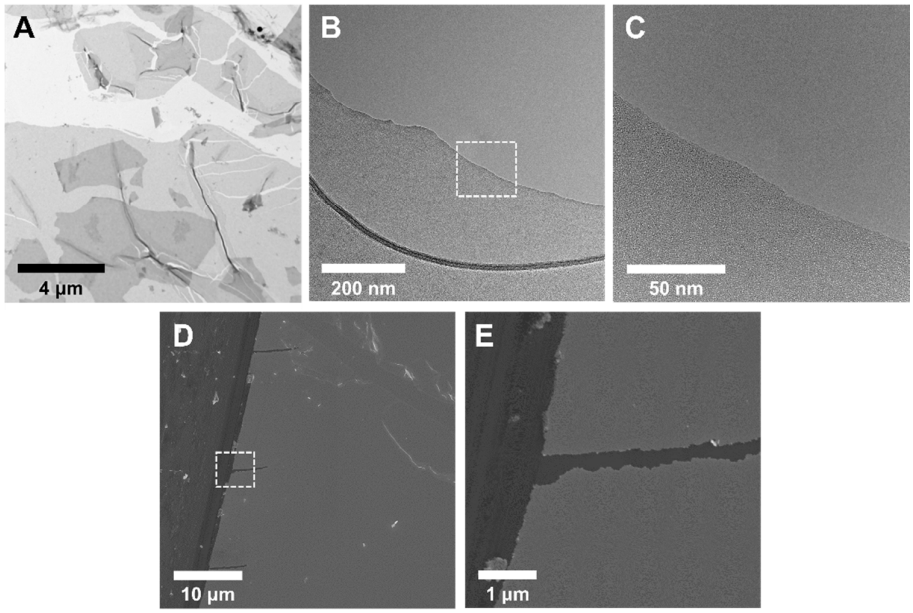

Figure S6. Imaging of YFCFY dimer sheets assembled at the air/water interface. (A) TEM image of the sheets (B, C) HR-TEM images of the sheet on a holey carbon grid (D, E) SEM images of the sheets on a silicon oxide substrate.

Low magnification image in Figure S6A, S6D, and S6E shows macroscopically uniform morphology of dimer sheets. Direct imaging of the dimer sheet on a holey carbon grid at high magnification clearly resolved its structural integrity showing that it is not composed of entangled networks of bundled fibrils (figure S6B and S6C). Despite its homogeneous 2D structure, it was difficult to obtain electron diffraction patterns and sharp peak from XRD analysis. This results may come from destructive damage by electron beam (when electron beam was focused on small area, the sheets tore up) or lack of long range ordering after drying though its integrity is sustained.

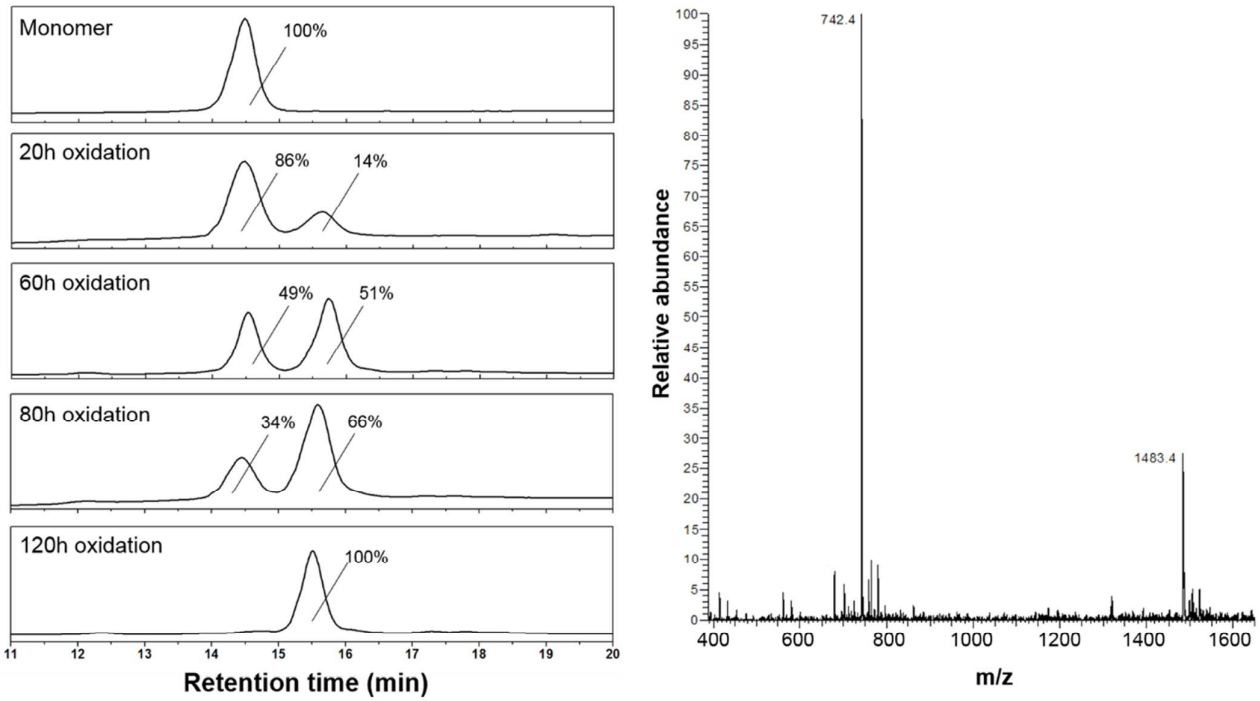

Figure S7. High Performance Liquid Chromatography (HPLC) results and Electrospray Ionization Mass Spectrometry (ESI-Mass) data of the second peak (15.5 min) in HPLC. In ESI mass result, the m/z peak at 1483.4 is of dimer YFCFY, the peak at 742.4 is of the monomer YFCFY. Monomer m/z peak was originated from molecules whose disulfide bonding was broken during ionization step in the mass analysis.

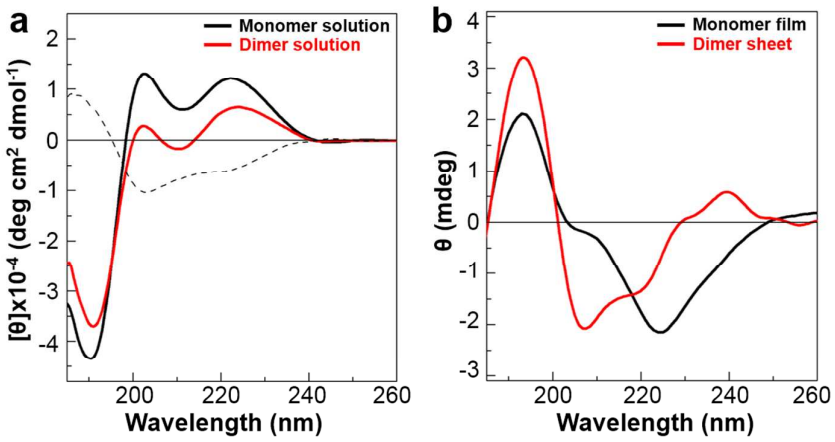

Figure S8. Circular dichroism (CD) analysis of YFCFY peptide. (a) CD spectra of 300 μM YFCFY monomer and 150 μM YFCFY dimer in water. The dashed curves are obtained by graphical subtraction of the spectra of dimer solution from that of monomer solution. (b) CD spectra of monomer film and dimer sheet directly transferred to a quartz cuvette by the stamping method. The solid CD spectra are expressed in degree of ellipticity (θ) without concentration terms and the solution CD spectrum are expressed in converted molar ellipticity ([θ]).

As shown in Figure S8a, the solution of monomer and dimer both exhibits two positive peaks at 202 nm and 224 nm. This CD spectra are not similar to typical CD spectra of the conformations such as α-helix, β-sheet, and random coil. The two positive peaks can arise due to contributions from aromatic chromophores, such as phenols and benzenes, which cause interference with the signal from the amides depending on the local environment.[1-3] The CD measurements of poly-L-tyrosine in a helical conformation revealed that there is the positive Cotton effect from the tyrosine side chain at 225 nm.[4] In addition, strong positive band contribution from tyrosine side chains at approximately 225 nm has been observed in several proteins.[4-7] The positive peak located at approximately 200 nm originated from the amide π-π* transition and L_a, L_b transition of tyrosine and phenylalanine.[5] Therefore, the positive peaks located at 202 nm and 224 nm in our systems may arise from tyrosine, phenylalanine, and the amide transition. These strong positive peaks near 202 nm and 225 nm from tyrosine and phenylalanine are overlapped with the negative broad peaks centered on 207 nm and 222 nm from n-π* transition of the α-helical peptide bonds. As a result, a relatively weak negative peak near 215 nm, instead of showing two minima at 207 and 222 nm, is considered as one of the characteristics of PLT and TRP with a right-handed alpha-helical conformation. YFCFY dimer and monomer solution both exhibits strong positive peak around 202 and 225 nm, and only dimer solution shows negative peak at 212 nm which is similar to the reported right-handed α-helical TRP and PLT. With the assumption that the contribution of the peptide chromophores and the aromatic contribution are additive, the spectrum characteristic of a non-aromatic right-handed α-helix is obtained clearly by subtracting the spectra of dimer solution from that of monomer solution.(Figure S8a) The resulting spectrum (dashed) shows double minima at 204 and 221 nm. Within this context, the solution CD spectra can support the presence of right-handed α-helical conformation although the CD spectra are different from the typical characteristics of α-helix.

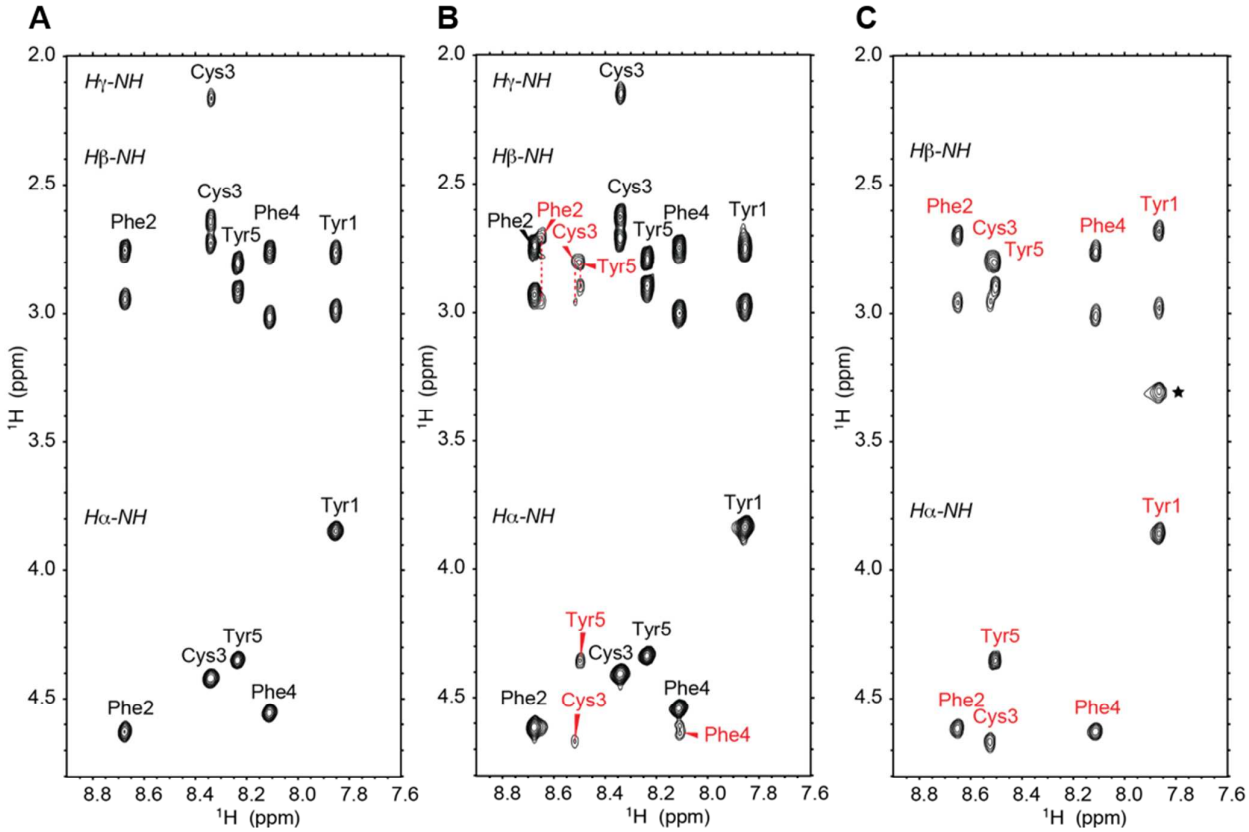

Figure S9. 2D TOCSY NMR spectra of YFCFY peptide after (A) 0 h, (B) 24h and (C) 48 h of oxidation in DMSO at 60 ºC. Spectra show the correlation between alpha, beta, and gamma protons and amide protons. With increasing reaction time, formation of dimeric YFCFY generates new resonances for Cys3, Phe4, and Tyr5 (B, red). No resonance for Cys3 gamma proton clearly proves the formation of a disulfide bond between Cys residues (C). Star is only shown in the dimeric form of YFCFY that is originated from the TOCSY correlation between the amide proton of Tyr1 and its aromatic proton in the phenol ring.

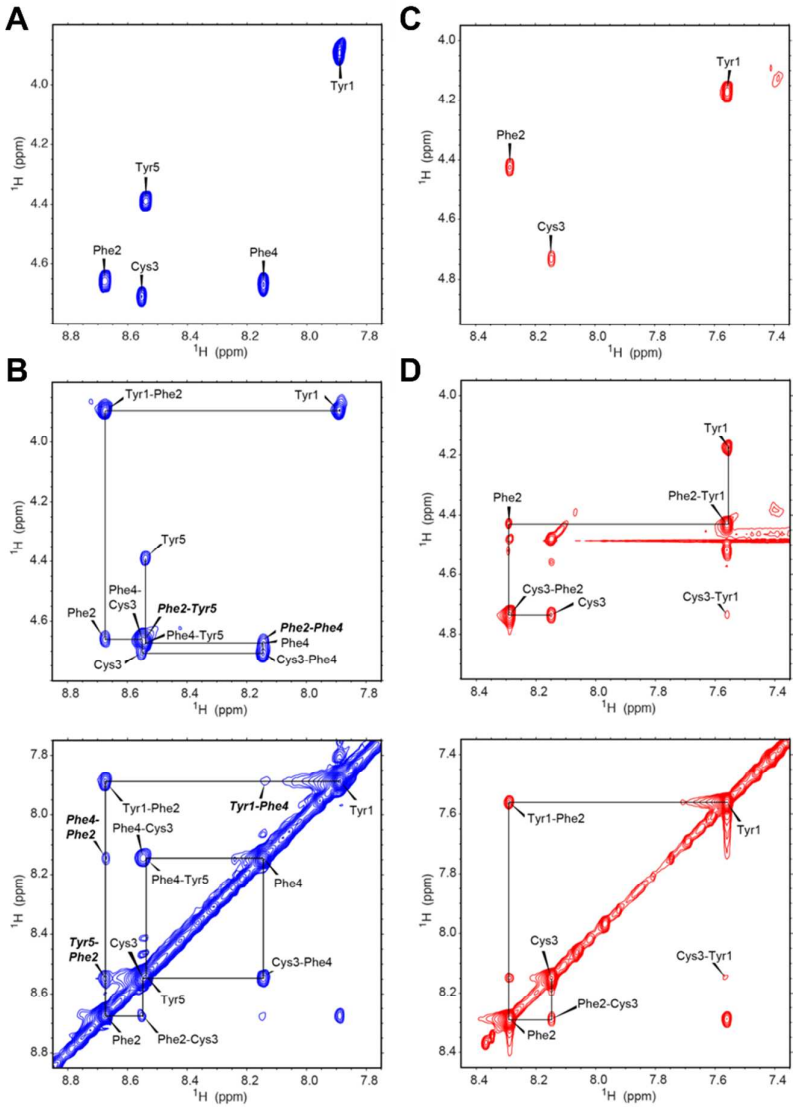

Figure S10. 2D NMR analysis of YFCFY dimeric peptides in 100% (blue) or 50% DMSO (red). (A,C) 2D TOCSY spectra shows the correlations between amide and alpha protons. (B,D) The NOEs between amide and alpha protons (top) and between amide protons (bottom) are shown in 2D NOESY spectra. In 50% DMSO (red), the resonances for only Tyr1, Phe2, and Cys3 appear, indicating that the structure of YFCFY dimer peptide in aqueous solution forms a different conformation.

The folding of YFCFY dimer structure is disturbed when the peptide is mixed with aqueous buffer (50% sodium phosphate pH 7.2 and 50% DMSO). The peak intensities of the spectra in the mixed solution became weaker than in 100% DMSO, and only three amino acid residues Tyr1, Phe2 and Cys3 are observed in the NMR correlation spectra. In 2D NOESY, the sequential NOEs of YFCFY dimer are observed only for Tyr1 through Cys3, and the NOE patterns are also different from those observed in 100% DMSO. These spectral changes is probably caused by the formation of invisible aggregation of YFCFY dimers in aqueous solution, where most of the consisting amino acids contain hydrophobic side chains. The aggregation between peptides seem to occur through Phe4 and Tyr5, since the resonances of Phe4 and Tyr5 are muchly broadened. The small and broadened residual peaks also indicates forming a multiple conformation of YFCFY dimers due to aggregations., which are contrast to previous NMR results from the experiments using 100% DMSO. In 100% DMSO solution, dimer exhibits not only strong sequential NOEs between neighboring amide protons but additional non-sequential NOEs such as those associated with Tyr1-Phe4, Phe2-Phe4, and Phe2-Tyr5 (Figure S10B). These connectivities represent typical conformation of helix, or more specifically 3_{10} helix[8,9].

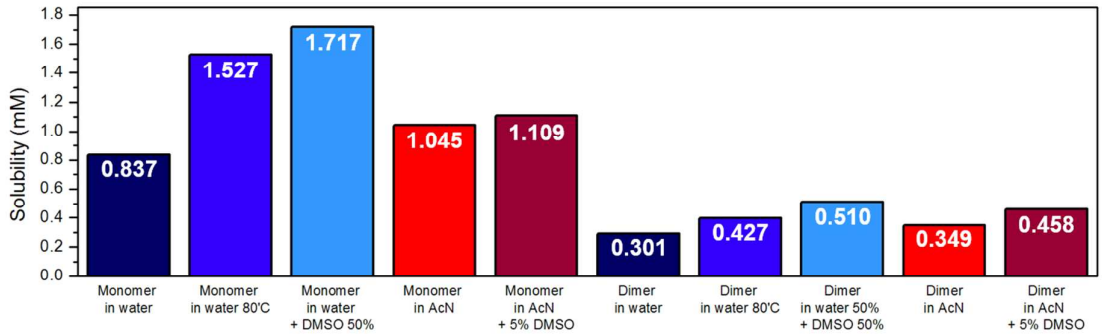

Figure S11. Solubility chart of YFCFY monomer and dimer in different conditions**.**

Ref 1) Beychok, S. Circular Dichroism of Biological Macromolecules. *Science* **1966**, *154*, 1288–1299.

Ref 2) Goodman, M.; Toniolo, C.; Peggion, E. Conformational Aspects of Polypeptides. XXIX. Conformational Assignments for Some Aromatic Polypeptides by Far-UV Cotton Effects. New Results. *Biopolymers* **1968**, *6*, 1691–1695.

Ref 3) Fretto, L.; Strickland, E. H. Effect of Temperature upon the Conformations of Carboxypeptidase A (Anson), A_{γ}^{Leu}, A_{γ}^{Val}, and $A_{\alpha+\beta}$. *Biochim. Biophys. Acta* **1971**, *235*, 473–488.

Ref 4) Beychok, S.; Fasman, G. D. Circular Dichroism of Poly-L-Tyrosine*. *Biochemistry* **1964**, *3*, 1675–1678.

Ref 5) Chen, Y. H.; Lo, T. B.; Yang, J. T. Optical Activity and Conformation of Cobra Neurotoxin. *Biochemistry* **1977**, *16*, 1826–1830.

Ref 6) Cameron, D. L.; Tu, a T. Characterization of Myotoxin a from the Venom of Prairie Rattlesnake (Crotalus Viridis Viridis). *Biochemistry* **1977**, *16*, 2546–2553.

Ref 7) Timasheff, S. N.; Bernardi, G. Studies on Acid Deoxyribonuclease: VII. Conformation of Three Nucleases in Solution. *Arch. Biochem. Biophys.* **1970**, *141*, 53–58.

Ref 8) Bax, A. Two-Dimensional NMR and Protein Structure. *Annu. Rev. Biochem*. **1989**, 58, 223–256.

Ref 9) Zarbock, J.; Clore, G. M.; Gronenborn, A. M. Nuclear Magnetic Resonance Study of the Globular Domain of Chicken Histone H5: Resonance Assignment and Secondary Structure. *Proc. Natl. Acad. Sci. U.S.A.* **1986**, 83, 7628–7632.